Second-order piezoelectricity in wurtzite III-N semiconductors

Joydeep Pal, Geoffrey Tse, Vesel Haxha, and Max A. Migliorato*
School of Electrical and Electronic Engineering, University of Manchester, United Kingdom

Stanko Tomić
Joule Physics Laboratory, School of Computing, Sciences and Engineering, University of Salford, United Kingdom
(Received 8 June 2011; revised manuscript received 15 July 2011; published 30 August 2011)

First- and second-order piezoelectric coefficients for all binary group-III nitride (III-N) wurtzite semiconductors are calculated using *ab initio* density functional theory. The method used allows the simultaneous determination of spontaneous and strain-induced polarization within the same framework. Although the linear coefficients are similar to all existing values reported in the literature, all spontaneous polarization terms are substantially smaller than the currently proposed values. Second-order coefficients also change the total strain-induced polarization significantly. We compare the predictions obtained using these coefficients with data in superlattice structures comprising binary nitride semiconductors and by including composition dependence with all available experimental data on III-N ternary alloys. We show that, unlike existing models, our calculated piezoelectric coefficients and nonlinear model provide a close match to the internal piezoelectric fields of quantum well and superlattice structures.

DOI: 10.1103/PhysRevB.84.085211 PACS number(s): 73.61.Ey, 77.65.Bn, 77.65.Ly, 78.67.De

I. INTRODUCTION

The piezoelectric (PZ) effect in bulk III-V semiconductors arises from lack of inversion symmetry along particular crystallographic directions[1–3] and is important in devices as diverse as light-emitting diodes, lasers, power electronics, transducers and micropositioners.[4] Among III-V semiconductors, the group-III nitride (III-N) family is the one for which the strongest influence of piezoelectricity on the optical and electrical properties is observed.[5,6] This is because the piezoelectric coefficients (PZCs) are typically one order of magnitude larger than other III-V materials[7] and because the polarization vector is in most cases parallel to the growth direction.[8] The calculation of PZ properties in semiconductors is often affected by uncertainties in the correct values of the PZCs and, in the case of wurtzite (WZ) crystals, by the additional problem of determining the spontaneous polarization ($P_{\rm sp}$) component.[7] The linear approximation is also a possible source of error, as second-order effects of significant magnitude have been reported in zincblende (ZB) InGaAs[9,10] and in III-N semiconductors.[11–15] However, for III-N second-order PZCs have not yet been reported, making it difficult to assess the influence of second-order piezoelectricity in nanostructures.

To resolve the issue of calculating the spontaneous and strain-induced PZ effect beyond the linear model, we present a semiempirical method in which a physical model is used to represent the influence of atomic displacement and atomic charge on the creation of an electrical dipole in a WZ crystal, while the variations of these quantities as a function of strain are calculated in the framework of *ab initio* density functional theory (DFT).

II. THE PHYSICAL MODEL

To evaluate all linear and nonlinear coefficients, we determined the total polarization resulting from both spontaneous and strain-induced polarization using the method that we previously showed to produce accurate predictions for InGaAs.[9,16] The method comprises a semiempirical approach with the PZ polarization given by the sum of a direct dipole contribution and a bond contribution, as originally proposed by Harrison,[17]

$$P_{\hat{x}_i} = \frac{Z_H^* \delta r + 2\alpha_p\left(1-\alpha_p^2\right)\sum_{q=1}^{4}(\vec{r}.\hat{x}_i)\,\delta R_q}{2\Omega}, \qquad (1)$$

where $\hat{x}_i$ is the Cartesian direction; δr is the displacement vector of cations in respect of anions from the ideal position (i.e., the situation in which all bonds in the tetrahedron are equal to one another); r_q and δR_q are the distance and displacement (deviation from the ideal position) vectors of the nearest-neighbor q from the atom at the center of the tetrahedron, respectively; α_p is the bond polarity; and Ω is the atomic volume. Borrowing from the language of tight binding, Z_H^* is the atomic charge—generally different from the transverse effective charge, which has its direct equivalent in the dynamic effective charge, or Born charge (Z^*), calculated with the density functional perturbation theory (DFPT).

We showed in our previous work on ZB GaAs and InAs[9,16] that Z_H^* needs to be roughly 25% of the value of the dynamic effective charge (Z^*) to obtain values of the PZ polarization in agreement with experiment. The effective charge was used in our model to evaluate the bond polarity: $Z^* = -\Delta Z + 4\alpha_p + 4\alpha_p\,(1-\alpha_p{}^2)$, with $\Delta Z = 1$.

The atomic charge Z_H^* was instead determined so that, once α_p and the elastic deformation have been determined in the limit of small strain, the experimental value of one of the PZCs (we chose e_{31}) is correctly reproduced:

$$P_{\rm strain} = e_{31}\cdot\varepsilon_{\parallel} = P_{\rm Tot} - P_{\rm sp} = \frac{Z_H^*\cdot(\delta r-\delta u)+2\alpha_p\left(1-\alpha_p^2\right)\cdot\sum_{q=1}^{4}(\vec{r}_q\cdot\hat{x}_i)\delta R_q}{2\Omega}. \qquad (2)$$

III. DFT CALCULATIONS

The elastic deformation and Z^*, for both the bulk and the strained cases, were evaluated by using plane-wave pseudopotential, with pseudopotentials derived with the Troullier-Martin scheme,[18] with density functional theory in the local density approximation (DFT-LDA),[19] and with density functional perturbation theory (DFPT), with instead pseudopotentials derived with the Hamann scheme,[20] within the CASTEP[21] code. Single-particle orbitals expressed in a plane-wave basis set with kinetic energy of up to 10^3 eV, and Brillouin zone summations of up to $10\times10\times6$ Monkhorst-Pack k-point grids[22] were sufficient to converge the simulations below a remaining error of $\sim$1%.

The dynamic effective charge was computed from the Born charge matrix, studied via the Berry phase approach[23] by applying a finite electric field perturbation in periodic boundary conditions. The matrix was then diagonalized, and an average of the eigenvalues was taken as the effective charge. Both its bulk and its strain dependence were determined in the same way.

WZ crystals are characterized by three independent quantities: the a in-plane lattice parameter, the c off-plane lattice parameter, and the u deformation from the ideal structure. The u parameter is at the origin of the P_{sp} effect, because even in the absence of external strain the tetrahedrons are asymmetric, resulting in only three of the four bonds being equal in length to one another. Strain-induced polarization arises from additional modifications of the cation positions relative to the anions under the effect of external pressure. One major advantage of the present approach is that both the spontaneous and the strain-induced polarization effects are described within the same model; hence, the results we present for the PZCs and the P_{sp} are uniquely linked. Furthermore only one PZC (e_{31}) was used as input, whereas the other ones (e_{33} and e_{15}) are calculated.

IV. LINEAR PZC

The DFT-calculated equilibrium values for a, c, and u are presented in Table I for GaN, AlN, and InN, together with Z^* and the resulting bond polarity α_p. The results of our calculations yielded values similar to those reported earlier.[7,24–26] In the same table, we report the experimental values of e_{31} used to fit Z_H^* in our models, together with the obtained values of Z_H^* which are much smaller than those of Z^*, as explained earlier.

The prediction of our model shows substantial agreement with reported experimental values of e_{33} for bulk III-N (data in brackets). However, for e_{15} our predictions are always slightly larger than previously proposed values. Also, the sign of e_{15}, as predicted by our model, is negative for all III-N materials studied. In the literature, both positive[27,28] and negative[29,30] values of e_{15} have been reported, but we identified this as being the result of a misprint contained in Muensit *et al.*[27] when reporting the experimental values from Tsubouchi and Mikoshiba.[29] The frequently cited work of Bernardini and Fiorentini[28] reported the value of Muensit *et al.*[27] rather than the original experimental work, and because many authors referred to their work[28] when listing PZCs, the error propagated. The compilation from Vurgaftman and Meyer[31] also contains the erroneous positive sign.

V. SPONTANEOUS POLARIZATION

The most striking difference between our predictions and earlier reports (data in brackets in Table I) is the values of the P_{sp}, for which no direct experimental data are available. The calculation of the P_{sp} followed exactly the methodology used for determining the PZCs once the value of Z_H^* was identified. The values that we calculated are between 25% and 65% of the values reported in the literature.[28,30] This is not surprising, because often the P_{sp} has been calculated using a simple dipole model with charges equal to the transverse effective charge (Z^*). The simple dipole model is equivalent to the first term in our model derived from Harrison's original formulation.[17] Because we use Z_H^*, the atomic charge, in our model, whereas earlier work tended to use Z^* (which is roughly three to four times larger), our values are proportionally smaller. The problem that calculating both PZCs and P_{sp} using

TABLE I. Physical parameters of III-Ns (GaN, AlN, and InN) calculated in this work. Comparisons with other calculated or experimental values are in brackets.

Parameters	GaN	AlN	InN
a (Å)	3.155	3.063	3.523
c (Å)	5.149	4.906	5.725
u (Å)	0.376	0.382	0.377
Z^*	2.583	2.553	2.850
α_p	0.517	0.511	0.578
Z_H^*	0.70	0.85	0.65
P_{sp} (C/m^2)	-0.007 (-0.029_{th})[28]	-0.051 (-0.081_{th})[28]	-0.012 (-0.032_{th})[28]
e_{31} (C/m^2)	-0.55 (-0.55_{exp})[27]	-0.6 (-0.6_{exp})[27]	-0.55 (-0.55_{exp})[42]
e_{33} (C/m^2)	1.05 (1.12_{exp})[27]	1.47 (1.50_{exp})[27]	1.07 (0.95_{exp})[42]
e_{15} (C/m^2)	-0.57 (-0.38_{th})[30]	-0.6 (-0.48_{exp})[29]	-0.65 (-0.44_{th})[30]
e_{311} (C/m^2)	6.185	5.850	5.151
e_{333} (C/m^2)	-8.090	-10.750	-6.680
e_{133} (C/m^2)	1.543	4.533	1.280

Z^* leads to grossly overestimated PZCs has been pointed out by Bernardini and Fiorentini.[28] Furthermore, we note the existence of experimentally extrapolated values of the P_{sp},[32–34] which are substantially smaller than those given in the literature.[28,30]

VI. STRAIN DEPENDENCE OF THE POLARIZATION

We also studied the strain dependence of the total polarization (strain induced plus P_{sp}) to determine whether the second-order PZ effect in the strain has relevance to WZ crystals. Nonlinear polarization effects have already been reported for the III-N semiconductors[11,35]; however, to the best of our knowledge, no comprehensive list of second-order PZCs has been reported.

Our previous work on ZB InGaAs[9,16] showed that second-order effects in the strain arise from a nonlinear displacement of the interpenetrating cation and anion face-centered cubic sublattices. Such nonlinearity was revealed in our previous work, even using DFT-LDA. Furthermore, the effective charges and hence the bond polarity appear to have a second-order dependence on the strain, though the effect is weaker. In WZ crystals, such behavior is also present, leading overall to a nonlinear behavior of the total polarization.

In Fig. 1, we show the total polarization as a function of combinations of parallel and perpendicular strain (varying from -0.1 to 0.1), calculated with our model (circles) and compared with the predictions from the linear model (dashed lines) using parameters compiled by Bernardini and Fiorentini.[28]

The first obvious difference between the two models is the reduced values of the P_{sp}, which offset the various lines of constant stress along the c-axis. Furthermore, our model has second-order terms that result in the bowing of the various lines, as expected from a second-order model with quadratic dependence. For parallel strain in the (0001) plane not exceeding ± 0.08 and large strain along the c-axis (i.e., perpendicular strain), our model always predicts significantly reduced positive values of total polarization for the tensile case, and greatly increased values for the compressive case, compared to the linear model. As an example, a thin-film GaN layer pseudomorphically grown on AlN would be strained by -3% in the growth plane ($\varepsilon_{//}$) and by $+6\%$ along the c-axis ($\varepsilon_{\perp}$), resulting in a linear polarization of $+0.095$ C/m^2 but a substantially lower second-order value of $+0.06$ C/m^2. This is clearly a large correction and cannot be neglected.

If we removed the P_{sp} and only considered strain-induced PZ polarization, for small strains the results of the two models would always coincide, as expected. However, with larger strain the second-order terms become more important and deviations between the two models become more pronounced. It is only when the different values of the P_{sp} term are introduced that we notice that for large compressive strain in the plane, for example, the two models appear to coincide. However, this is purely coincidental and has no physical significance. What has significance is that our model predicts a much larger negative and a smaller positive range of attainable PZ fields for strain in the range $\pm 10\%$

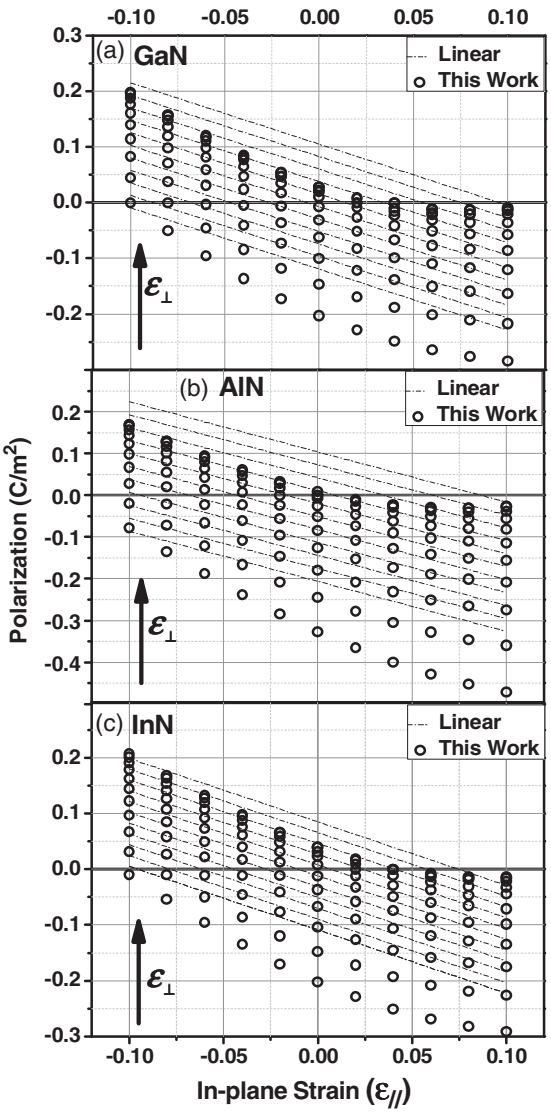

FIG. 1. Comparison of the total polarization as a function of perpendicular and parallel strain calculated in this work (circles) and using the linear model with parameters from Ref. 28 (dashed lines). The perpendicular strain varies from -0.1 to 0.1 in steps of 0.02.

VII. SECOND-ORDER PZC

By fitting our data with a second-order polynomial, we obtained second-order PZCs for quadratic terms in the strain containing parallel and perpendicular strain components (but not for those containing shear coefficients). The results are presented in Table I, where the subscripts 311, 333, and 133 refer, respectively, to a double strain in the plane, a double strain perpendicular to the plane, and the combination of both parallel and perpendicular strain. The coefficients given in Table I allow us to express the strain dependence of the magnitude of the total PZ polarization in the direction orthogonal to the growth plane as

$$P_{\mathrm{Tot}} = P_{\mathrm{sp}} + e_{33}\varepsilon_{\perp} + 2e_{31}\varepsilon_{\parallel} + e_{311}\varepsilon_{\parallel}^2 + e_{333}\varepsilon_{\perp}^2 + e_{133}\varepsilon_{\parallel}\varepsilon_{\perp} \tag{3}$$

We have not evaluated the second-order dependence of the polarization due to shear strain in the growth direction or

growth plane, connected to the PZC e_{15}. Such dependence could have a potential impact on nanostructures such as quantum dots[6] but not on two-dimensional thin films, which are the focus of this work, for which Eq. (3) is valid.

VIII. COMPARISON WITH EXPERIMENTAL RESULTS ON BINARY MATERIALS

To test the validity of our method and the PZCs obtained (listed in Table I), we compared our results with the experimental values for AlN/GaN superlattices.[36–39]

For this comparison, we evaluated the field in the AlN and GaN regions (conventionally referred to as the barrier b and well region w, respectively) using the well-known superlattice equations[34]

$$F_z^w = \frac{\left(P_{\mathrm{SP}}^b + P_{\mathrm{PZ}}^b - P_{\mathrm{SP}}^w - P_{\mathrm{PZ}}^w\right)}{\epsilon^w + \epsilon^b\,(L_w/L_b)} \tag{4}$$

and

$$F_z^b = -\frac{L_w}{L_b} F_z^w. \tag{5}$$

In Eqs. (4) and (5), the spontaneous and strain-induced polarizations (P_{sp} and P_{PZ}) combine to give a resulting field in the z direction of growth. The field F also depends on the dielectric constant of the material (ϵ) and the relative lengths L_w and L_b of the well and barrier material, respectively.

For the relative dielectric constant, we used values of 10.0, 8.5, and 15.3 for GaN, AlN, and InN, respectively, while using a linear interpolation between binary values for the alloys.

Comparison between our calculated fields (to the first and second orders) in the well region (GaN) and experimental values for several superlattices differing only in the L_w/L_b ratio are presented in Table II. We also show the results of the calculations using the widely used parameters of Bernardini and Fiorentini[28] (previous work). For this material combination, the second-order effect is small, because the GaN region is unstrained for growth on GaN on sapphire.

Hence, in this case, the field is mainly produced by the difference in P_{sp}, which with our parameters is 0.044 C/m^2. Our calculated values are in excellent agreement with all available experimental data, with the exception of one source,[38] where the agreement is nevertheless satisfactory (the case of $L_w/L_b = 0.8 \pm 0.26/2.8 \pm 0.52$). Furthermore, our model appears to produce much closer agreement compared to using the parameters from previous work.[28]

Another independent theoretical work[40] has attempted to calculate the barrier and well fields in the framework of DFT (in the generalized gradient approximation and in the self interaction corrected scheme). The authors' predictions, based on calculating the interface electrostatic potential difference in superlattice structures, also appear consistent with both the experimental data and our calculated values (Table II). The substantial agreement confirms the correctness of our PZCs for GaN and AlN. In particular, it validates the proposed lower values of the P_{sp} term, which is probably the most interesting outcome of our model.

We attempted a similar comparison with superlattice structures comprising InN/GaN layers. Unfortunately, we could not find any experimental data to verify our predictions. However, theoretical values[41] have been calculated with the method used by Cui *et al.*[40] The calculated values for the three methods discussed are listed in Table II.

The difference between the values of the P_{sp} for InN and those for GaN is only 0.005 C/m^2; hence, this case is a stronger test for the strain-induced polarization. It is difficult to make conclusions based on the obtained data, because our model does not always agree with that of Shieh *et al.*[41] The two models seem to agree either for the barrier or for the well values but not for both. It is possible that the structures used in the calculations differ by some aspect, but we cannot draw any conclusions here other than, again, that the linear model

TABLE II. Experimental and calculated values of the PZ field in various quantum wells comprising binary GaN, AlN, and InN combinations. The calculated values in this work have been obtained to both first and second orders for comparison. We also calculated (previous work) the corresponding values using the first-order parameters of Bernardini and Fiorentini (Ref. 28). The last column provides the estimates of the ratio of the well width to the barrier width used in the superlattice equations (Ref. 32).

Quantum well	Experiment	This work (to second order)	This work (to first order)	Previous work	L_w/L_b
	(MV/cm)	(MV/cm)	(MV/cm)	(MV/cm)	
GaN/AlN	10.2[36]	10.30	10.10	10.65	2.6/100[36]
GaN/AlN	8.0[37]	8.06	7.91	8.43	2.5/6[37]
GaN/AlN	10.0 ± 1.0[38]	9.00 ± 0.50	8.80 ± 0.5	6.00 ± 1.00	$(0.8 \pm 0.26)/(2.8 \pm 0.52)$[38]
GaN/AlN	5.04[39]	5.06	4.95	4.76	2.3/1.9[39]
	$(5.19/4.76_{\mathrm{th}})$[40]				
GaN/AlN	6.07[39]	6.07	5.98	6.55	1.4/1.9[39]
	(6.09_{th})[40]				
InN/GaN	$9.25_{\mathrm{th(InN)}}$[41]	9.62	8.29	6.93	4.7/6[41]
	$8.13_{\mathrm{th(GaN)}}$[41]	8.24	7.10	5.90	
InN/GaN	$5.21_{\mathrm{th(InN)}}$[41]	6.61	6.10	5.85	7/4[41]
	$11.17_{\mathrm{th(GaN)}}$[41]	12.2	9.79	7.89	
InN/GaN	$3.99_{\mathrm{th(InN)}}$[41]	7.11	6.50	5.70	9.3/6[41]
	$8.52_{\mathrm{th(GaN)}}$[41]	11.51	10.05	7.33	
InN/GaN	$6.32_{\mathrm{th(InN)}}$[41]	9.32	8.13	7.2	7/8[41]
	$6.84_{\mathrm{th(GaN)}}$[41]	8.70	7.57	5.84	

TABLE III. Experimental and calculated values of the PZ field in various quantum wells comprising AlGaN/GaN and InGaN/GaN alloys. Experimental values for the GaN/InGaN structures were digitally extracted from Fig. 3 of Ref. 42. The calculated values have been obtained with the first- and the second-order parameters from this work and with the parameters from Bernardini and Fiorentini (Ref. 28, previous work), in both cases including the parabolic alloy dependence (Ref. 15). In brackets, for comparison, we also show the values obtained including a simple linear interpolation of the PZ parameters. The last column contains the values of the ratio of the well width to the barrier width used in the superlattice equations (Ref. 32).

Quantum well	Experiment	This work (to second order)	This work (to first order)	Previous work	L_w/L_b
	(MV/cm)	(MV/cm)	(MV/cm)	(MV/cm)	
$Al_{0.17}Ga_{0.83}N/GaN$	0.76[32]	0.760 (1.010)	0.775	1.205 (1.730)	3/50[32]
$Al_{0.65}Ga_{0.35}N/GaN$	2.00[33]	2.090 (2.350)	2.130	2.170 (2.590)	6/3[33]
$GaN/In_{0.06}Ga_{0.94}N$	0.61[42]	0.606 (0.610)	0.594	0.544 (0.530)	3/3
$GaN/In_{0.09}Ga_{0.91}N$	1.00[42]	0.997 (0.980)	0.980	0.766 (0.756)	3/3
$GaN/In_{0.11}Ga_{0.89}N$	1.33[43]	1.325 (1.310)	1.290	1.210 (1.180)	3/3[43]
$GaN/In_{0.12}Ga_{0.88}N$	1.60[42]	1.603 (1.610)	1.575	1.500 (1.450)	3/6
$GaN/In_{0.22}Ga_{0.78}N$	3.09[42]	3.097 (3.120)	3.000	3.132 (3.231)	3/8

using parameters from Bernardini and Fiorentini[28] leads to substantial differences from our calculated values of the field.

IX. COMPARISON WITH EXPERIMENTAL RESULTS ON ALLOYS

Given that a significant amount of experimental data for AlGaN/GaN and InGaN/GaN quantum wells exists, the validity of our model can be further tested. A complication of treating alloys is that a significant parabolic dependence in the composition for all PZCs is present.[15] To test our parameters quantitatively, we have therefore introduced a parabolic alloy dependence in all our coefficients, including the second-order ones. The procedure we used was to apply to our parameters the same percentage deviation of the $Al_{0.5}Ga_{0.5}N$ and $In_{0.5}Ga_{0.5}N$ from the linearly interpolated values given in Ambacher *et al.*[15] for the classic model of Bernardini and Fiorentini.[28] Then we could easily fit a parabolic dependence in essence equivalent to that given in Ambacher *et al.*[15]

Using the corresponding parameters that define the quadratic dependence on alloy composition (Table IV), we then compared directly the values of the PZ field in the quantum well region reported for a variety of quantum well sizes and compositions for both AlGaN/GaN[32,33] and InGaN/GaN[42] structures. The reported values of the PZ field in quantum wells are not direct measurements but rather values derived from electro-optical characterization of confined levels. Again, our comparison is based on calculating the PZ fields in the quantum well region using Eqs. (4) and (5).

A comparison among experimental values of the PZ field in different quantum wells, the predictions obtained with the parameters from Bernardini and Fiorentini,[28] and those obtained with the second-order parameters of this work, with and without the parabolic dependence on the alloy composition, is presented in Table III. The parabolic dependence on alloy composition is essential in obtaining PZ fields in the range of values of experiment, as evidenced by comparing the data obtained with and without (data in brackets) the use

TABLE IV. Quadratic dependence on alloy composition for ternary nitride alloys ($Al_xGa_{1-x}N$, $In_xGa_{1-x}N$). The parameters are for the equation $Y = Ax^2 + Bx + C$.

System	Y	A	B	C
$Al_xGa_{1-x}N$	P_{sp}	−0.025	−0.019	−0.007
	e_{31}	0.064	−0.114	−0.550
	e_{33}	0.141	0.279	1.050
	e_{311}	−0.674	−1.000	6.185
	e_{333}	1.055	3.715	−8.090
	e_{133}	−0.340	−2.650	1.543
$In_xGa_{1-x}N$	P_{sp}	−0.001	−0.005	−0.007
	e_{31}	−0.368	0.368	−0.550
	e_{33}	0.119	−0.099	1.050
	e_{311}	−0.635	−1.669	6.185
	e_{333}	1.182	−0.228	−8.090
	e_{133}	−0.226	−0.489	1.543

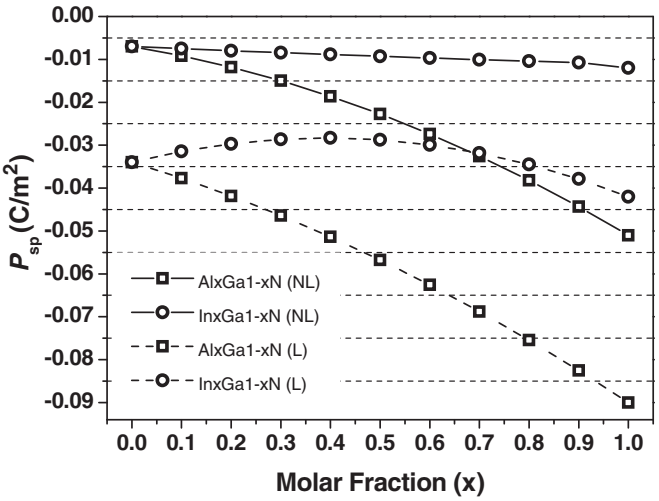

FIG. 2. Comparison of the P_{sp} for the $Al_xGa_{1-x}N$ (squares) and $In_xGa_{1-x}N$ (circles) alloys as a function of the molar fraction x, calculated in this work (solid lines for the nonlinear model, or NL) and calculated using the linear model (L) with parameters from Ref. 15 (dashed lines for the linear model). The quadratic dependence in the molar fraction, with parameters from Table IV, was used to evaluate the data within the solid lines.

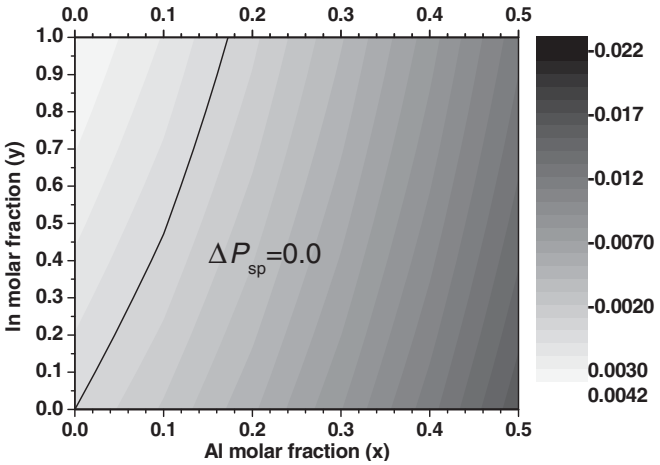

FIG. 3. Mapping of the difference in the P_{sp} between $Al_xGa_{1-x}N$ and $In_yGa_{1-y}N$ for $x \leqslant 0.5$ and $0 < y < 1$. The solid line illustrates the region in which such a difference vanishes ($0 < x < 0.17$).

of a quadratic equation with parameters listed in Table IV for our model and those from Ambacher *et al.*[15] for values listed under previous work. However it is also obvious that a substantial improved agreement with experimental data was obtained when using our model compared to the widely used one of Bernardini and Fiorentini.[28]

Just like for the binary materials, the AlGaN/GaN structures are more sensitive to a difference in P_{sp}, whereas in the InGaN/GaN structures the strain-induced polarization and hence the second-order coefficients play a more important role. This is confirmed by the tendency of the difference between first and second order to increase as the In content is increased, a consequence of sharply increasing strain.

The closeness of our predictions for the field in the well region and the experimentally reported data indicates strongly that our calculated PZCs for InN appear to be verified in real structures.

X. MATCHING SPONTANEOUS POLARIZATION IN NITRIDE ALLOYS

As an interesting case, we now discuss the values of the P_{sp} in the ternary alloys AlGaN and InGaN. In Fig. 2, we compare the values of the P_{sp} for the $Al_xGa_{1-x}N$ (squares) and those for $In_xGa_{1-x}N$ (circles) alloys as a function of the molar fraction, as evaluated in this work (solid lines) and as calculated using the linear model with parameters from Ref. 15 (dashed lines). The quadratic dependence in the molar fraction for the P_{sp} values in this work was introduced using the parameters from Table IV. First, the model used for the dashed lines predicts that only In-rich InGaN with In content of at least 80% would exhibit the same P_{sp} as an AlGaN alloy. For this to happen, the Al content would have to be low, up to ∼20%.

The data presented in the solid lines, which use our reduced values of the P_{sp} term, show that instead this equality can be easily achieved at low In and Al contents. In Fig. 3, we show the mapping of the difference in P_{sp} between $Al_xGa_{1-x}N$ and $In_yGa_{1-y}N$ for $x \leqslant 0.5$ and y between 0 and 1. A line exists where such a difference vanishes for values of x between 0% and 17%. Because of the inherent difficulty of growing In-rich InGaN alloys the fact that it is possible to find vanishing P_{sp} differences for low-enough In and Al fractions means the possibility of designing layers where, according to Eqs. (4) and (5), the PZ field is entirely due to the strain-induced polarization and is reduced, compared to having materials with a difference in the P_{sp} terms.

XI. CONCLUSIONS

We have calculated both the P_{sp} and the first- and second-order PZCs in the framework of *ab initio* DFT and DFPT and in conjunction with the semiempirical formulation of Harrison.[17]

Compared with previous calculations, which used only the linear theory of piezoelectricity and large values of the P_{sp}, our model, where a significant role of second-order piezoelectricity and much smaller values of the P_{sp} are proposed, provides better agreement with available experimental data of the PZ field in the quantum well regions for various III-N materials and their alloys.

Furthermore, we showed that our model predicts that, by choosing particular values of the molar fractions in AlGaN and InGaN alloys, it is possible to match the P_{sp} terms and reduce the total PZ field to the strain-induced one alone. This could have applications in the design of optoelectronic devices.

ACKNOWLEDGMENTS

The authors thank E. P. O'Reilly, S. Schulz, and M. Caro of the Tyndall National Institute in Cork, Ireland, for extremely valuable discussions.

*m.migliorato@physics.org

[1] R. M. Martin, Phys. Rev. B **5**, 1607 (1972).
[2] W. G. Cady, *Piezoelectricity* (McGraw-Hill, New York, 1946).
[3] L. C. Lew Yan Voon and M. Willatzen, J. Appl. Phys. **109**, 031101 (2011).
[4] S. Nakamura and G. Fasol, *The Blue Laser Diode: GaN Based Light Emitters and Lasers* (Springer-Verlag, Berlin, 1997).
[5] A. D. Andreev and E. P. O'Reilly, Phys. Rev. B **62**, 15851 (2000).
[6] S. Tomić and N. Vukmirović, Phys. Rev. B **79**, 245330 (2009).
[7] F. Bernardini, V. Fiorentini, and D. Vanderbilt, Phys. Rev. B **56**, R10024 (1997).
[8] E. T. Yu, X. Z. Dang, P. M. Asbeck, S. S. Lau, and G. J. Sullivan, J. Vac. Sci. Technol. B **17**, 1742 (1999).
[9] M. A. Migliorato, D. Powell, A. G. Cullis, T. Hammerschmidt, and G. P. Srivastava, Phys. Rev. B **74**, 245332 (2006).
[10] G. Bester, X. Wu, D. Vanderbilt, and A. Zunger, Phys. Rev. Lett. **96**, 187602 (2006).

[11]G. Vaschenko, C. S. Menoni, D. Patel, C. N. Tomé, B. Clausen, N. F. Gardner, J. Sun, W. Götz, H. M. Ng, and A. Y. Cho, Phys. Status Solidi B **235**, 238 (2003).
[12]D. Cai and G-Y. Guo, J. Phys. D: Appl. Phys. **42**, 185107 (2009).
[13]K. Shimada, T. Sota, K. Suzuki, and H. Okumura, Jpn. J. Appl. Phys. **37**, Pt.2,12A (1998).
[14]G. Vaschenko, D. Patel, C. S. Menoni, N. F. Gardner, J. Sun, W. Götz, C. N. Tomé, and B. Clausen, Phys. Rev. B **64**, 241308 (2001).
[15]O. Ambacher, J. Majewski, C. Miskys, A. Link, M. Hermann, M. Eickhoff, M. Stutzmann, F. Bernardini, V. Fiorentini, V. Tilak, B. Schaff, and L. F. Eastman, J. Phys.: Condens. Matter **14**, 3399 (2002).
[16]R. Garg, A. Hüe, V. Haxha, M. A. Migliorato, T. Hammerschmidt, and G. P. Srivastava, Appl. Phys. Lett. **95**, 041912 (2009).
[17]W. A. Harrison, *Electronic Structure and Properties of Solids* (Dover Publications, New York, 1989).
[18]N. Troullier and J. L. Martins, Phys. Rev. B **43**, 1993 (1991).
[19]J. P. Perdew and A. Zunger, Phys. Rev. B **23**, 5048 (1981).
[20]D. R. Hamann, Phys. Rev. B **40**, 2980 (1989).
[21]S. J. Clark, M. D. Segall, C. J. Pickard, P. J. Hasnip, M. J. Probert, K. Refson, and M. C. Payne, Z. Kristallogr. **220**, 567 (2005).
[22]H. J. Monkhorst and J. D. Pack, Phys. Rev. B **13**, 5188 (1976).
[23]M. V. Barry, Proc. R. Soc. Lond. A **392**, 45 (1984).
[24]A. Zoroddu, F. Bernardini, P. Ruggerone, and V. Fiorentini, Phys. Rev. B **64**, 045208 (2001).
[25]S. Y. Karpov, Phys. Status Solidi C **7**, 1841 (2010).
[26]J. Xin, Y. Zheng, and E. Shi, Appl. Phys. Let. **91**, 112902 (2007).
[27]S. Muensit, E. M. Goldys, and I. L. Guy, Appl. Phys. Lett. **75**, 4133 (1999).
[28]F. Bernardini and V. Fiorentini, Appl. Phys. Lett. **80**, 4145 (2002).
[29]K. Tsubouchi and N. Mikoshiba, IEEE Trans. Sonics Ultrason. **SU-32**, 634 (1985).
[30]K. Shimada, Jpn. J. Appl. Phys. **45**, L358 (2006).
[31]I. Vurgaftman and J. R. Meyer, J. Appl. Phys. **94**, 3675 (2003).
[32]M. Leroux, N. Grandjean, J. Massies, B. Gil, P. Lefebvre, and P. Bigenwald, Phys. Rev. B **60**, 1496 (1999).
[33]N. Suzuki and N. Iizuka, Jpn. J. Appl. Phys. **38**, L363 (1999).
[34]S.-H. Park and S.-L. Chuang, Appl. Phys. Lett. **76**, 1981 (2000).
[35]D. Cai and G.-Y. Guo, J. Phys. D: Appl. Phys. **42**, 185107 (2009).
[36]C. Adelmann, E. Sarigiannidou, D. Jalabert, Y. Hori, J.-L. Rouvie‘re, B. Daudinc, S. Fanget, C. Bru-Chevallier, T. Shibata, and M. Tanaka, Appl. Phys. Lett. **82**, 4154 (2003).
[37]A. Helman, M. Tchernycheva, A. Lusson, E. Warde, F. H. Julien, Kh. Moumanis, G. Fishman, E. Monroy, B. Daudin, D. Le Si Dang, E. Bellet-Amalric, and D. Jalabert, Appl. Phys. Lett. **83**, 5196 (2003).
[38]M. Tchernycheva, L. Nevou, L. Doyennette, F. H. Julien, E. Warde, F. Guillot, E. Monroy, E. Bellet-Amalric, T. Remmele, and M. Albrecht, Phys. Rev. B **73**, 125347 (2006).
[39]C. Buchheim, R. Goldhahn, A. T. Winzer, G. Gobsch, U. Rossow, D. Fuhrmann, A. Hangleiter, F. Furtmayr, and M. Eickhoff, Appl. Phys. Lett. **90**, 241906 (2007).
[40]X. Y. Cui, D. J. Carter, M. Fuchs, B. Delley, S. H. Wei, A. J. Freeman, and C. Stampfl, Phys. Rev. B **81**, 155301 (2010).
[41]C. C. Shieh, X. Y. Cui, B. Delly, and C. Stampfl, J. Appl. Phys. **109**, 083721 (2011).
[42]A. Hangleiter, F. Hitzel, S. Lahmann, and U. Rossow, Appl. Phys. Lett. **83**, 1169 (2003).
[43]H. Kollmer, I. Seo Im, S. Heppel, J. Off, F. Scholz, and A. Hangleiter, Appl. Phys. Lett. **74**, 82 (1999).